Published in final edited form as:
Ann Plast Surg. 2013 September ; 71(3): 308–315. doi:10.1097/SAP.0b013e31828b02fb.

A Novel Pilot Study Using Spatial Frequency Domain Imaging to Assess Oxygenation of Perforator Flaps During Reconstructive Breast Surgery

John T. Nguyen, MD[*], **Samuel J. Lin, MD**[*], **Adam M. Tobias, MD**[*], **Sylvain Gioux, PhD**[†], **Amaan Mazhar, PhD**[†,§], **David J. Cuccia, PhD**[‖], **Yoshitomo Ashitate, MD**[†,¶], **Alan Stockdale, MEd**[†], **Rafiou Oketokoun, MEng**[†], **Nicholas J. Durr, PhD**[†], **Lorissa A. Moffitt, MS**[†], **Anthony J. Durkin, PhD**[§], **Bruce J. Tromberg, PhD**[†,§], **John V. Frangioni, MD, PhD**[‡,#], and **Bernard T. Lee, MD, MBA**[*]

[*]Division of Plastic and Reconstructive Surgery, Department of Surgery, Beth Israel Deaconess Medical Center, Boston, MA

[†]Division of Hematology/Oncology, Department of Medicine, Beth Israel Deaconess Medical Center, Boston, MA

[‡]Department of Biomedical Engineering, University of California Irvine

[§]Beckman Laser Institute, Technology Incubator Office, Irvine, CA

[‖]Modulated Imaging Inc, Technology Incubator Office, Irvine, CA

[¶]Division of Cancer Diagnostics and Therapeutics, Hokkaido University Graduate School of Medicine, Sapporo, Japan

[#]Department of Radiology, Beth Israel Deaconess Medical Center, Boston, MA.

Abstract

Introduction—Although various methods exist for monitoring flaps during reconstructive surgery, surgeons primarily rely on assessment of clinical judgment. Early detection of vascular complications improves rate of flap salvage. Spatial frequency domain imaging (SFDI) is a promising new technology that provides oxygenation images over a large field of view. The goal of this clinical pilot study is to use SFDI in perforator flap breast reconstruction.

Methods—Three women undergoing unilateral breast reconstruction after mastectomy were enrolled for our study. The SFDI system was deployed in the operating room, and images acquired over the course of the operation. Time points included images of each hemiabdominal skin flap before elevation, the selected flap after perforator dissection, and after microsurgical transfer.

Results—Spatial frequency domain imaging was able to measure tissue oxy-hemoglobin concentration (ctO_2Hb), tissue deoxyhemoglobin concentration, and tissue oxygen saturation (stO_2). Images were created for each metric to monitor flap status and the results quantified throughout the various time points of the procedure. For 2 of 3 patients, the chosen flap had a higher ctO_2Hb and stO_2. For 1 patient, the chosen flap had lower ctO_2Hb and stO_2. There were no perfusion deficits observed based on SFDI and clinical follow-up.

Reprints: Bernard T. Lee, MD, MBA, Beth Israel Deaconess Medical Center, Harvard Medical School, 110 Francis St, Suite 5A, Boston, MA 02215. blee3@bidmc.harvard.edu..

Conflicts of interest: None of the authors have a conflict of interest to declare.

Conclusions—The results of our initial human pilot study suggest that SFDI has the potential to provide intraoperative oxygenation images in real-time during surgery. With the use of this technology, surgeons can obtain tissue oxygenation and hemoglobin concentration maps to assist in intraoperative planning; this can potentially prevent complications and improve clinical outcome.

Keywords

perforator flap; breast reconstruction; microsurgery; perfusion mapping; near-infrared imaging; spatial frequency domain imaging

Abdominal-based, autologous flaps are well-established options for breast reconstruction after mastectomy.[1–5] Commonly used options include the pedicled transverse rectus abdominis myo-cutaneous, free transverse rectus abdominis myocutaneous, and deep inferior epigastric perforator (DIEP) flaps.[6–11] The dissection of these flaps requires adequate perfusion to ensure success; in addition, the advent of microsurgical reconstruction is further associated with potential risks and complications of microsurgery.

Technological advances are necessary to improve flap perfusion and minimize donor-site morbidity. In particular, vessel thrombosis, partial and total flap loss, and fat necrosis are associated with poor outcomes.[6,12] As early recognition has been shown to lead to improved flap salvage and success,[12] it is vital that vascular compromise is detected effectively to expedite surgical and therapeutic intervention for free flap salvage. Currently, the standard of care to monitor perfusion is the clinical observation of skin warmth, color, capillary refill, and dermal bleeding. This subjective approach leads to a wide degree of variability in reported rates of flap loss.[13]

Methods to identify early flap failure intraoperatively include thermal, flow, perfusion, and oxygen monitoring.[14] Each method has limitations precluding widespread use. We provide here a review of each method, purposely excluding computed tomographic angiography and magnetic resonance angiography because they are not widely used intraoperatively.

- Thermal monitoring using noncontact infrared imaging has been previously evaluated, particularly in the form of dynamic infrared thermography. However, this technique requires cooling the surface of the flap (cold challenge), which can prove challenging to implement routinely into clinical practice.[15,16]
- Flow monitoring by Doppler effect (performed either using ultra-sound waves or optically)[17–20] and by laser speckle imaging[21,22] has been used to assess blood flow in microsurgically anastomosed arteries and veins. However, such methods are typically noisy, can require vessels to be exposed, can require contact, suffer from surrounding vessel interference, and provide limited information about presence or absence of flow.
- Perfusion assessment, or angiography, can be performed intraoperatively using optical fluorescence imaging.[23,24] This method attempts to monitor flaps by characterizing perfusion at the skin or superficial capillary level.[25,26] Although this method can reliably visualize perforator arteries in flaps, it remains by nature superficial and requires the injection of an exogenous contrast agent.
- Tissue oximetry probes have been introduced for flap monitoring, as they are easy to use and are relatively inexpensive.[27–30] The main advantage of this approach is direct measurement of tissue oxygenation, a surrogate for perfusion and indicator of tissue status. Such methods are intuitive to most clinicians as the technology is similar to pulse oximetry, which was introduced in the 1970s.[31–33] These methods

rely on light absorption from tissue endogenous constituents such as oxyhemoglobin, deoxyhemoglobin, water, and lipids.[34,35] Several clinically approved probes are currently commercially available and have reached daily clinical practice in some hospitals. Note that the oxygen saturation levels measured with tissue oximetry probes reflect both venous and arterial blood oxygen saturation (normal level around 70%), whereas pulse oximetry measures arterial oxygen saturation only (normal level over 90%).

Two major approaches exist to implement these methods, namely, local contact probes and noncontact imaging devices. Local probes require contact (and in some cases, the use of a matching gel), provide local readings of tissue status, and are therefore less useful in detecting areas of potential failure and perfusion deficits because prior knowledge of the location of a defect is required. In addition, such probes can be sensitive to pressure and movement, can be noisy, and can require long stabilization times. Imaging techniques have the advantage of providing wide-field, noncontact monitoring of an entire flap in a single image. However, most methods to date require long acquisition and/or postprocessing times that makes them sensitive to movement and preclude their use as real-time feedback monitoring devices.

An ideal technology would allow clinicians to determine tissue status over a large area. Oxygenation imaging provides the ability to identify areas of ischemia, using well-known metrics by clinicians and without prior knowledge of the location of a defect. Multispectral wide-field imaging is emerging as an attractive, noninvasive imaging modality.[36–38] Spatial frequency domain imaging (SFDI) is a noncontact optical imaging method that allows for fast acquisition (<1 second) and accurate interrogation of tissue optical properties over large fields of view (>100 cm^2).[39,40] This method, when performed at multiple near-infrared (NIR) wavelengths allows measurement of concentrations of tissue constituents (namely, oxyhemoglobin, deoxyhemoglobin, lipids, and water) using Beer's law at depths typically less than 5 mm.[41–43] Briefly, the SFDI system consists of a multispectral NIR light source and a projector to illuminate the field with invisible spatially modulated patterns, a camera to acquire images, and a computer to process and display the images to the surgeon. The main advantage of this approach over other continuous wave multispectral wide-field imaging methods is that absorption of tissues is separated from scattering through measurement and not through empirical assumptions.

Our group has previously validated a clinically compatible SFDI system for intraoperative oxygenation imaging during porcine skin flap, bowel, and liver vascular occlusion comparing extracted oxygenation maps with a clinically approved oxygenation probe (ViOptix, Fremont, Calif).[43] This previous study presented the detailed design of the imaging system, its validation during preclinical experiments and its translation into the clinic. In the current study, we present the results obtained with our SFDI system during our 3 patient, first-in-human, pilot study of flap oxygenation imaging during reconstructive breast surgery.

METHODS

SFDI Clinical System

The SFDI system used in this study has been optimized for intraoperative use. It is based on the Fluorescence Assisted Resection and Exploration (FLARE) clinical imaging system[23] on which a projector and a multispectral NIR source have been integrated allowing the performance of SFDI acquisitions over a 16 × 12-cm field of view at a 45-cm working distance. This SFDI system meets all requirements for mechanical and electrical safety as defined in IEC 60601. Briefly, 1 SFDI acquisition consists of projecting 6 wavelengths onto

the surgical field (670, 730, 760, 808, 860, and 980 nm) with 3 sets of patterns. These wavelengths have been selected to permit rapid and reliable oxygenation imaging.[44] One set of pattern permits profilometry measurement and is used to correct for the sample's surface profile variations.[45] Two sets of patterns are used to extract optical properties. The acquisition is performed simultaneously on 2 NIR cameras, allowing the acquisition of 2 wavelengths at a time. Images acquired in real time during surgery are then processed to extract maps of ctO_2Hb, tissue deoxyhemoglobin concentration (ctHHb), and tissue oxygen saturation (stO_2). A schematic and an actual picture of the SFDI system are provided in Figure 1. Extensive details about the FLARE system and the SFDI clinical system can be found elsewhere.[23,43]

First-in-Human Pilot Study

The clinical pilot study was approved by the institutional review board of the Beth Israel Deaconess Medical Center and was performed in accordance with the ethical standards of the Helsinki Declaration of 1975. The institutional review board deemed the SFDI system a “nonsignificant risk” device. Study subjects were women undergoing unilateral or bilateral mastectomy and reconstruction with a microsurgical DIEP flap. Informed consent was obtained before surgery. Patient demographics include age range from 41 to 65 years, with 2 patients undergoing immediate unilateral reconstruction and 1 delayed unilateral reconstruction. Flap weights ranged from 326 to 890 g and perforators were chosen based on clinical observation (see Table 1).

Trained personnel deployed the imaging system into the operating room. The system was draped in sterile fashion using a shield/drape combination that could be applied by a single person (scrub nurse). After draping, the imaging head entered the sterile field and was positioned at a fixed distance. Images were acquired to extract profile information and optical properties at several wavelengths, as described previously.

The standard imaging protocol included 4 sets of SFDI measurements. The first 2 SFDI measurements were taken before flap elevation by positioning the system 45 cm over each hemiabdomen. On the basis of standard practice, the surgeon chose to dissect 1 set of vessels (from the right or left side of the abdomen). A third SFDI measurement was taken after dissection of the vessels through the intramuscular course and isolation of the selected perforator vessels and vascular pedicle. The flap was then transferred to the chest and a microsurgical anastomosis was performed attaching the deep inferior epigastric artery and vein to the internal mammary vessels. A final measurement was performed using SFDI at this time point. Results from the SFDI measurements were not accessible to the operating surgeons in this feasibility study, thereby not altering the standard of care.

Once discharged from the hospital, patients were seen during the routine course of follow-up. If no emergent complications occurred, patients were seen at 1 week after discharge, then at 6 weeks, 3 months, and 6 months after surgery. The reconstructed breast and surgical sites were evaluated at the time of the follow-up with emphasis on perfusion issues such as fat necrosis and partial flap loss.

RESULTS

SFDI Oxygenation Imaging Results

Four SFDI measurements were taken during the DIEP flap procedure. These measurements were taken at crucial time points, including each abdominal hemiflap (discarded and chosen abdominal flap), images of the chosen flap after elevation (postflap elevation), and after microsurgical attachment (postflap transplant). Extracted concentration maps of tissue oxyhemoglobin (ctO_2Hb), tissue deoxyhemoglobin (ctHHb), and tissue oxygen saturation

(stO_2) are shown for each patient in Figures 2, 3, and 4 (top, middle, and bottom row, respectively).

Patient 1

Abdominal Flaps—The SFDI maps showed that both flaps had good oxyhemoglobin and oxygen saturation levels initially. Both abdominal flaps showed good tissue oxygen saturation levels (76% and 74%, respectively) in a region of interest chosen in the middle of the flap (dashed black square in Fig. 2). In this case, the right flap was chosen for harvest and transplantation. The chosen flap had a higher ctO_2Hb level compared to the discarded flap (157 and 111 μM, respectively) and a higher ctHHb level (49 and 38 μM, respectively).

Postelevation—As the vascular pedicle was isolated and the chosen flap elevated, tissue oxygen saturation decreased from 76% to 74% in our chosen flap, with a 20% decrease in ctO_2Hb (126 μM) and 12% decrease in ctHHb (43 μM).

Posttransplantation—Once the flap was transplanted, measurements showed tissue oxygen saturation decreasing from 74% to 69%, with a 26% decrease in ctO_2Hb (100 μM) and a slight increase in ctHHb (45 μM).

Patient 2

Abdominal Flaps—The SFDI maps showed both flaps with good oxyhemoglobin and oxygen saturation levels initially. Both abdominal flaps had identical tissue oxygen saturation levels at 71% in a region of interest chosen in the middle of the flap (dashed black square in Fig. 3). Here the left flap was chosen for harvest and transplantation. The chosen flap had a higher ctO_2Hb level compared to the discarded flap (123 and 104 μM, respectively) and a higher ctHHb level (51 and 41 μM, respectively).

Postelevation—As the vascular pedicle was isolated and the chosen flap elevated, tissue oxygen saturation increased from 71% to 73% in our chosen flap, with a 31% decrease in ctO_2Hb (85 μM) and 39% decrease in ctHHb (31 μM).

Posttransplantation—Once the flap was transplanted, measurements showed relatively unchanged tissue oxygen saturation at 72%, with a 28% increase in ctO_2Hb (109 μM) and a 32% increase in ctHHb (41 μM).

Patient 3

Abdominal Flaps—The SFDI maps showed both flaps with low oxyhemoglobin and oxygen saturation levels initially. The left flap showed tissue oxygen saturation at 68%, whereas the right flap showed tissue oxygen saturation at 55% in a region of interest chosen in the middle of the flap (dashed black square in Fig. 4). Here the right flap was chosen for harvest and transplantation. The chosen flap had a lower ctO_2Hb level compared to the discarded flap (78 and 84 μM, respectively) and a higher ctHHb level (63 and 38 μM, respectively).

Postelevation—As the vascular pedicle was isolated and the right flap elevated, tissue oxygen saturation increased from 55% to 60%, with a 12% decrease in ctO_2Hb (69 μM) and 27% decrease in ctHHb (46 μM).

Posttransplantation—Once the right flap was transplanted, measurements showed a decrease in tissue oxygen saturation from 60% to 54%, with a 17% decrease in ctO_2Hb (57 μM) and a slight increase in ctHHb (48 μM).

Postoperative Follow-up—Our 3 patients were seen in clinic for follow-up at the time points described. Patients were examined for any flap perfusion issues and postoperative photographs were taken (Fig. 5). In all 3 patients, no vascular or perfusion complications were observed in follow-up. There were no areas of fat necrosis or partial flap loss identified postoperatively. All 3 flaps healed without any sequelae and the patients all went on to complete their reconstructive course.

Quantification of Results—Localized measurements from similar regions of interests (dashed black squares in Figs. 2–4) were quantified and their mean and standard deviation plotted (Fig. 6). Tissue oxyhemoglobin content, tissue deoxyhemoglobin content, and tissue oxygen saturation levels were evaluated for all 3 patients. Time points include comparison of chosen and discarded flap as well as the chosen flap postelevation and posttransplantation.

Tissue Oxyhemoglobin (ctO_2Hb)—All 3 patients had differences in ctO_2Hb between the 2 hemiflaps. In patients 1 and 2, the side with higher ctO_2Hb level was chosen for dissection and transfer (41% and 18% higher, respectively). In patient 3, the side with the lower ctO_2Hb level was chosen (7% lower). After elevation and vessel dissection, the flaps on all 3 patients demonstrated a decrease in ctO_2Hb (–20%, –31%, and –12%, respectively). After microsurgical anastomosis and flap transfer, ctO_2Hb varied from patient to patient but all showed lower levels compared to baseline before vessel dissection (–36%, –11%, and –27%, respectively).

Tissue Deoxyhemoglobin (ctHHb)—All 3 patients had differences in ctHHb between the 2 hemiflaps. The chosen flap in all 3 patients had a higher ctHHb level (+29%, +24%, and +66%, respectively). After flap elevation, the flaps on all 3 patients showed a decrease in ctHHb (–12%, –39%, and –27%, respectively). However, after flap transfer, there was a slight improvement in ctHHb level (+5%, +32%, and +4%, respectively), although not returning to baseline before vessel dissection.

Tissue Oxygen Saturation (stO_2)—In patient 1, the flap with higher stO_2 was chosen (76% vs 74%); in patient 2, the 2 flaps had the same level (71%); and in patient 3, the flap with the lower level was chosen (55% vs 68%). After flap elevation and vessel dissection, stO_2 remained consistent and was slightly lower in patient 1 (–3%), although increased in patients 2 and 3 (+3% and +9%, respectively). After flap transfer in patient 1, the flap showed a decrease in stO_2 compared to baseline levels (–9%), with little change in patients 2 and 3 (+1% and –2%, respectively).

DISCUSSION

In this article, we present the results from a first-in-human pilot study of a novel SFDI device to assess flap status with tissue oxygenation imaging. The imaging system was successfully deployed in 3 patients undergoing breast reconstruction surgery. We demonstrated the ability to provide wide-field maps of tissue constituents and tissue oxygen saturation in each patient over the entire flap and at various time points. This includes evaluation of both hemiflaps (comparing both left and right flaps), after pedicle dissection and elevation of flap, and after transplantation.

The use of this imaging system could potentially improve clinical outcomes as oxygenation imaging allows for immediate surgical intervention. During elevation of the flap, SFDI would allow for assistance in the selection of flap used for harvest. During the dissection of the perforators and the isolation of the vascular pedicle, SFDI would allow identification of potential areas of diminished perfusion. After transplantation and microsurgical

anastomosis, SFDI could allow for the immediate assessment of the flap status. The benefit to providing such measurements over large fields of view is the ability to identify areas of potential defect (hypoxia or ischemia) without prior indication for concern. Imaging at these time points may elicit immediate intervention whether it is the use of the contralateral flap, limiting the size of flap transferred, anticoagulation, or revision of the anastomosis.

In this study, the surgeon was blinded as to the results of the imaging system and clinical judgment was used during surgery to select the vessels and flap for harvest and transfer. For patients 1 and 2, SFDI confirms that the clinically chosen flaps for transplantation have higher oxygenation quantitatively with increased levels of oxyhemoglobin and oxygen saturation as compared with the discarded flap. However, for patient 3, SFDI suggests the discarded flap had better perfusion metrics, whereas the chosen flap was deemed clinically acceptable. Although these findings did not demonstrate clinical significance, knowledge of this information in patient 3 could have altered the course of surgery and may potentially improve outcomes in other cases.

The quantitative metrics identified with the SFDI system include tissue-level oxyhemoglobin, deoxyhemoglobin, and oxygen saturation. Importantly, the long-term postoperative clinical results from the transplanted flaps of our 3 patients correlated well with clinical results showing no areas of concern on our posttransplantation tissue oxygenation maps. Although large increases in deoxyhemoglobin are associated with compromised arterial perfusion and large increases in oxyhemoglobin associated with compromised venous drainage,[43] the thresholds for clinical perfusion deficits are still to be determined. In these 3 patients, although oxygen saturation was found to exhibit little variations, oxyhemoglobin and deoxyhemoglobin demonstrated larger variations throughout the course of dissection and transfer. In large animal studies from our laboratory, oxyhemoglobin and deoxyhemoglobin show distinct patterns of change that are more sensitive than oxygen saturation levels alone; these changes can potentially signal perfusion compromise at earlier time points.

Two distinct intraoperative patterns can be seen in our study (Fig. 6). In 1 pattern, seen in patients 1 and 2, higher oxyhemoglobin, deoxyhemoglobin, and oxygen saturation levels were seen in the chosen flap potentially demonstrating better overall perfusion. After elevation and microsurgical transfer, these levels were lower than baseline. The images obtained with SFDI correlated well with clinical assessment at the time of surgery in these patients with adequate tissue oxygen saturation levels (~70%), and high oxyhemoglobin concentration (150 μM), suggesting healthy flap status.

In contrast, a different pattern is seen in patient 3, which depicts a flap with lower oxyhemoglobin and higher oxygen saturation levels after flap dissection. In this patient, the chosen flap showed some equilibration after flap dissection as demonstrated by an increase in oxygen saturation. After elevation and microsurgical flap transfer, the oxyhemoglobin and oxygen saturation were below baseline as previously mentioned. As free flaps undergo a period of hypoxia once harvested and reperfused, this transient period of decreased oxygenation in the flap was observed in both patterns. It would be interesting to understand how these metrics equilibrate over time and determine thresholds for inadequate perfusion. Finally, it is interesting to note that all patients had a similar deoxyhemoglobin concentration pattern over the procedure, with a decreased level after elevation and an increased level after transplantation.

The imaging system described also has the capability for simultaneous NIR fluorescence angiography and SFDI. This combination could allow for the identification of vascular structures,[24,46,47] while also allowing for functional tissue perfusion mapping. Future work

is underway to understand the relationship between flap outcome, fluorescence angiography, and SFDI.

CONCLUSIONS

We have designed and validated a system that is capable of wide-field tissue constituents imaging (oxyhemoglobin, deoxyhemoglobin, and oxygen saturation) based on SFDI and multi-spectral principles. Our SFDI system was translated to clinical use in a first-in-human pilot study, where skin flap oxygenation was imaged during reconstructive breast surgery intraoperatively. Our study demonstrates proof of concept and feasibility of using SFDI for tissue perfusion mapping.

Acknowledgments

sources of funding: This study was funded by National Institutes of Health Grants R21-CA-129758, R01-CA-115296 (National Cancer Institute), and R01-EB-005805 (National Institute of Biomedical Imaging and Bioengineering). Additional support has been provided by the National Institutes of Health/NCRR Grant P41-RR01192 (Laser Microbeam and Medical Program), US Air Force Office of Scientific Research, Medical Free-Electron Laser Program Grants F49620-00-2-0371 and FA9550-04-1-0101, and the Beckman Foundation.

REFERENCES

1. Alderman AK, Kuhn LE, Lowery JC, et al. Does patient satisfaction with breast reconstruction change over time? Two-year results of the Michigan Breast Reconstruction Outcomes Study. J Am Coll Surg. 2007; 204:7–12. [PubMed: 17189107]
2. Guyomard V, Leinster S, Wilkinson M. Systematic review of studies of patients' satisfaction with breast reconstruction after mastectomy. Breast. 2007; 16:547–567. [PubMed: 18024116]
3. Hu ES, Pusic AL, Waljee JF, et al. Patient-reported aesthetic satisfaction with breast reconstruction during the long-term survivorship period. Plast Reconstr Surg. 2009; 124:1–8. [PubMed: 19568038]
4. Lee C, Sunu C, Pignone M. Patient-reported outcomes of breast reconstruction after mastectomy: a systematic review. J Am Coll Surg. 2009; 209:123–133. [PubMed: 19651073]
5. Yueh JH, Slavin SA, Adesiyun T, et al. Patient satisfaction in postmastectomy breast reconstruction: a comparative evaluation of DIEP, TRAM, latissimus flap, and implant techniques. Plast Reconstr Surg. 2010; 125:1585–1595. [PubMed: 20517080]
6. Allen RJ, Treece P. Deep inferior epigastric perforator flap for breast reconstruction. Ann Plast Surg. 1994; 32:32–38. [PubMed: 8141534]
7. Fujino T, Harashina T, Enomoto K. Primary breast reconstruction after a standard radical mastectomy by a free flap transfer. Case report. Plast Reconstr Surg. 1976; 58:371–374.
8. Hartrampf CR, Scheflan M, Black PW. Breast reconstruction with a transverse abdominal island flap. Plast Reconstr Surg. 1982; 69:216–225. [PubMed: 6459602]
9. Platt J, Baxter N, Zhong T. Breast reconstruction after mastectomy for breast cancer. CMAJ. 2011; 183:2109–2116. [PubMed: 22065359]
10. Serletti JM, Fosnot J, Nelson JA, et al. Breast reconstruction after breast cancer. Plast Reconstr Surg. 2011; 127:124e–135e.
11. Tonseth KA, Hokland BM, Tindholdt TT, et al. Quality of life, patient satisfaction and cosmetic outcome after breast reconstruction using DIEP flap or expandable breast implant. J Plast Reconstr Aesthet Surg. 2008; 61:1188–1194.
12. Disa JJ, Cordeiro PG, Hidalgo DA. Efficacy of conventional monitoring techniques in free tissue transfer: an 11-year experience in 750 consecutive cases. Plast Reconstr Surg. 1999; 104:97–101. [PubMed: 10597680]
13. Khouri RK, Cooley BC, Kunselman AR, et al. A prospective study of microvascular free-flap surgery and outcome. Plast Reconstr Surg. 1998; 102:711–721. [PubMed: 9727436]
14. Nahabedian MY. Overview of perforator imaging and flap perfusion technologies. Clin Plast Surg. 2011; 38:165–174. [PubMed: 21620143]

15. de Weerd L, Mercer JB, Setsa LB. Intraoperative dynamic infrared thermography and free-flap surgery. Ann Plast Surg. 2006; 57:279–284.
16. Itoh Y, Arai K. Use of recovery-enhanced thermography to localize cutaneous perforators. Ann Plast Surg. 1995; 34:507–511.
17. Hallock GG. Evaluation of fasciocutaneous perforators using color duplex imaging. Plast Reconstr Surg. 1994; 94:644–651. [PubMed: 7938287]
18. Hallock GG. Doppler sonography and color duplex imaging for planning a perforator flap. Clin Plast Surg. 2003; 30:347–357. v–vi. [PubMed: 12916592]
19. Yu P, Youssef A. Efficacy of the handheld Doppler in preoperative identification of the cutaneous perforators in the anterolateral thigh flap. Plast Reconstr Surg. 2006; 118:928–933. discussion 934-925. [PubMed: 16980853]
20. Schlosser S, Wirth R, Plock JA, et al. Application of a new laser Doppler imaging system in planning and monitoring of surgical flaps. J Biomed Opt. 2010; 15:036023. [PubMed: 20615025]
21. Boas DA, Dunn AK. Laser speckle contrast imaging in biomedical optics. J Biomed Opt. 2010; 15:011109. [PubMed: 20210435]
22. Huang YC, Ringold TL, Nelson JS, et al. Noninvasive blood flow imaging for real-time feedback during laser therapy of port wine stain birthmarks. Lasers Surg Med. 2008; 40:167–173. [PubMed: 18366081]
23. Gioux S, Choi HS, Frangioni JV. Image-guided surgery using invisible near-infrared light: fundamentals of clinical translation. Mol Imaging. 2010; 9:237–255. [PubMed: 20868625]
24. Lee BT, Hutteman M, Gioux S, et al. The FLARE intraoperative near-infrared fluorescence imaging system: a first-in-human clinical trial in perforator flap breast reconstruction. Plast Reconstr Surg. 2010; 126:1472–1481. [PubMed: 21042103]
25. Matsui A, Lee BT, Winer JH, et al. Quantitative assessment of perfusion and vascular compromise in perforator flaps using a near-infrared fluorescence-guided imaging system. Plast Reconstr Surg. 2009; 124:451–460. [PubMed: 19644259]
26. Matsui A, Lee BT, Winer JH, et al. Predictive capability of near-infrared fluorescence angiography in submental perforator flap survival. Plast Reconstr Surg. 2010; 126:1518–1527.
27. Benaron DA, Parachikov IH, Friedland S, et al. Continuous, noninvasive, and localized microvascular tissue oximetry using visible light spectroscopy. Anesthesiology. 2004; 100:1469–1475.
28. Keller A. A new diagnostic algorithm for early prediction of vascular compromise in 208 microsurgical flaps using tissue oxygen saturation measurements. Ann Plast Surg. 2009; 62:538–543. [PubMed: 19387157]
29. Lin SJ, Nguyen MD, Chen C, et al. Tissue oximetry monitoring in microsurgical breast reconstruction decreases flap loss and improves rate of flap salvage. Plast Reconstr Surg. 2011; 127:1080–1085. [PubMed: 21364410]
30. Rao R, Saint-Cyr M, Ma AM, et al. Prediction of post-operative necrosis after mastectomy: a pilot study utilizing optical diffusion imaging spectroscopy. World J Surg Oncol. 2009; 7:91. [PubMed: 19939277]
31. Mendelson Y. Pulse oximetry: theory and applications for noninvasive monitoring. Clin Chem. 1992; 38:1601–1607.
32. Middleton PM, Henry JA. Pulse oximetry: evolution and directions. Int J Clin Pract. 2000; 54:438–444.
33. Severinghaus JW. History and recent developments in pulse oximetry. Scand J Clin Lab Invest Suppl. 1993; 214:105–111. [PubMed: 8332844]
34. Delpy DT, Cope M. Quantification in tissue near-infrared spectroscopy. Philos Trans R Soc Lond B Biol Sci. 1997; 352:649–659.
35. Zonios G, Bykowski J, Kollias N. Skin melanin, hemoglobin, and light scattering properties can be quantitatively assessed in vivo using diffuse reflectance spectroscopy. J Invest Dermatol. 2001; 117:1452–1457. [PubMed: 11886508]
36. Attas M, Hewko M, Payette J, et al. Visualization of cutaneous hemoglobin oxygenation and skin hydration using near-infrared spectroscopic imaging. Skin Res Technol. 2001; 7:238–245. [PubMed: 11737819]

37. Vogel A, Chernomordik VV, Riley JD, et al. Using noninvasive multispectral imaging to quantitatively assess tissue vasculature. J Biomed Opt. 2007; 12:051604.
38. Zuzak KJ, Schaeberle MD, Lewis EN, et al. Visible reflectance hyperspectral imaging: characterization of a noninvasive, in vivo system for determining tissue perfusion. Anal Chem. 2002; 74:2021–2028. [PubMed: 12033302]
39. Dognitz N, Wagnieres G. Determination of tissue optical properties by steady-state spatial frequency-domain reflectometry. Lasers Med Sci. 1998; 13:55–65.
40. Cuccia DJ, Bevilacqua F, Durkin AJ, et al. Quantitation and mapping of tissue optical properties using modulated imaging. J Biomed Opt. 2009; 14:024012. [PubMed: 19405742]
41. Pharaon MR, Scholz T, Bogdanoff S, et al. Early detection of complete vascular occlusion in a pedicle flap model using quantitation spectral imaging. Plast Reconstr Surg. 2010; 126:1924–1935. [PubMed: 21124132]
42. Yafi A, Vetter TS, Scholz T, et al. Postoperative quantitative assessment of reconstructive tissue status in a cutaneous flap model using spatial frequency domain imaging. Plast Reconstr Surg. 2011; 127:117–130. [PubMed: 21200206]
43. Gioux S, Mazhar A, Lee BT, et al. First-in-human pilot study of a spatial frequency domain oxygenation imaging system. J Biomed Opt. 2011; 16:086015. [PubMed: 21895327]
44. Mazhar A, Dell S, Cuccia DJ, et al. Wavelength optimization for rapid chromophore mapping using spatial frequency domain imaging. J Biomed Opt. 2010; 15:061716. [PubMed: 21198164]
45. Gioux S, Mazhar A, Cuccia DJ, et al. Three-dimensional surface profile intensity correction for spatially modulated imaging. J Biomed Opt. 2009; 14:034045. [PubMed: 19566337]
46. Pestana IA, Coan B, Erdmann D, et al. Early experience with fluorescent angiography in free-tissue transfer reconstruction. Plast Reconstr Surg. 2009; 123:1239–1244. [PubMed: 19337092]
47. Komorowska-Timek E, Gurtner GC. Intraoperative perfusion mapping with laser-assisted indocyanine green imaging can predict and prevent complications in immediate breast reconstruction. Plast Reconstr Surg. 2010; 125:1065–1073. [PubMed: 20335859]

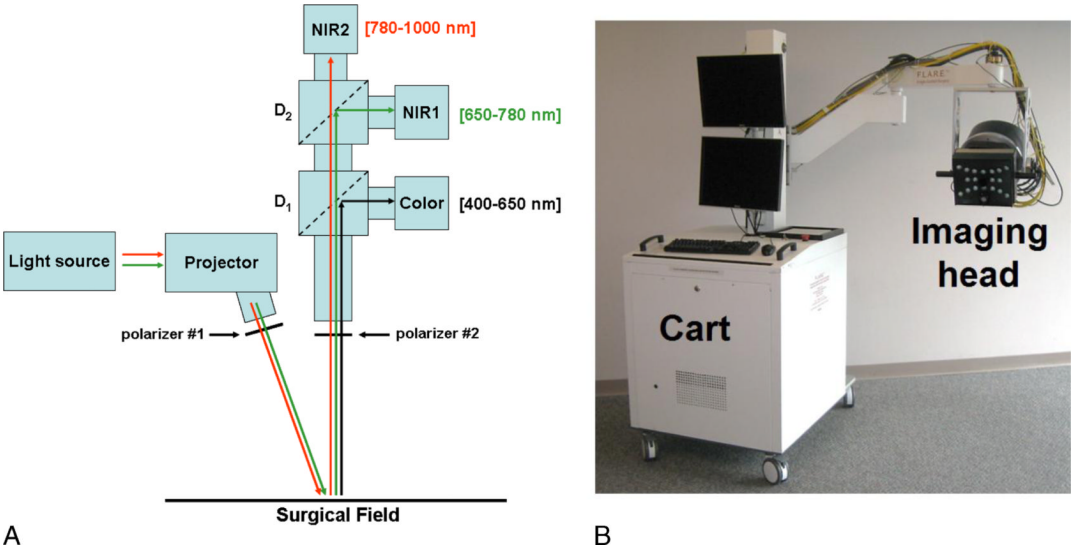

FIGURE 1.

SFDI system. A, Schematics of the system. The light from the NIR light source is coupled into the projector and patterns of NIR light projected onto the field. Wavelengths shown in green and red are collected by NIR cameras 1 and 2, respectively. B, Picture of the clinical imaging system composed of a cart containing the NIR light source, control electronics, computer, mast, and arm holding the adjustable imaging head.

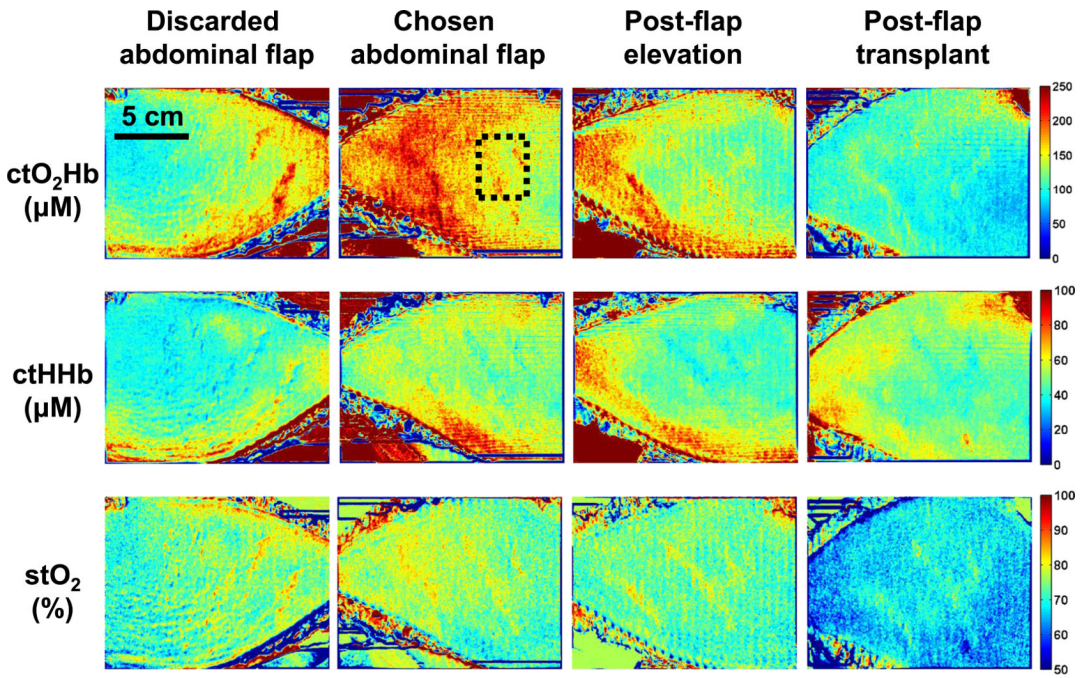

FIGURE 2.

SFDI oxygenation imaging results—Patient 1. Columns, from left to right, include abdominal skin flaps after preparation (discarded and chosen), skin flap after elevation, and skin flap after attachment (transplantation). The first row presents the concentration of tissue oxyhemoglobin (ctO_2Hb), the second row the concentration of tissue deoxyhemoglobin (ctHHb), and the third row the tissue oxygen saturation images (stO_2).

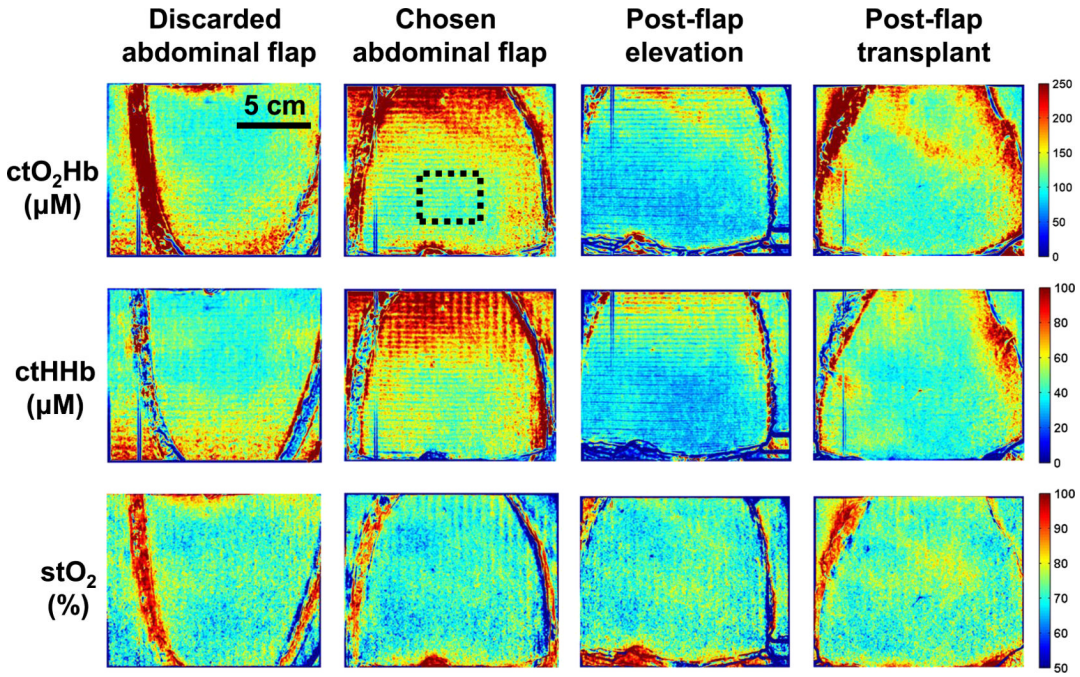

FIGURE 3.

SFDI oxygenation imaging results—Patient 2. Columns, from left to right, include abdominal skin flaps after preparation (discarded and chosen), skin flap after elevation, and skin flap after attachment (transplantation). The first row presents the concentration of tissue oxyhemoglobin (ctO_2Hb), the second row the concentration of tissue deoxyhemoglobin (ctHHb), and the third row the tissue oxygen saturation images (stO_2).

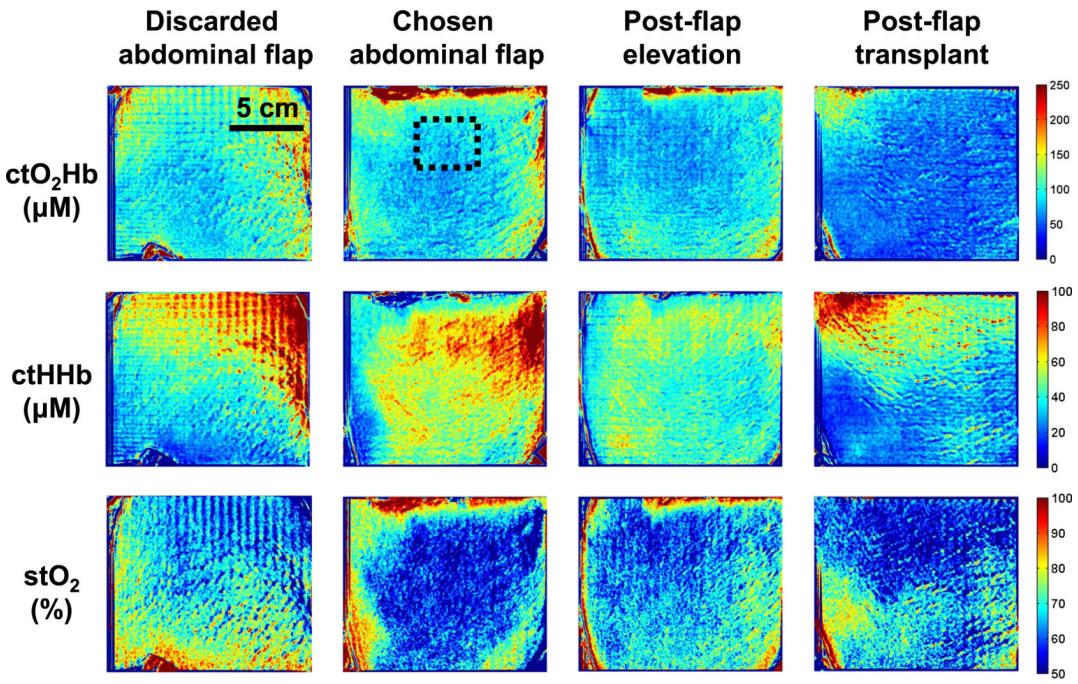

FIGURE 4.

SFDI oxygenation imaging results—Patient 3. Columns, from left to right, include abdominal skin flaps after preparation (discarded and chosen), skin flap after elevation, and skin flap after attachment (transplantation). The first row presents the concentration of tissue oxyhemoglobin (ctO_2Hb), the second row the concentration of tissue deoxyhemoglobin (ctHHb), and the third row the tissue oxygen saturation images (stO_2).

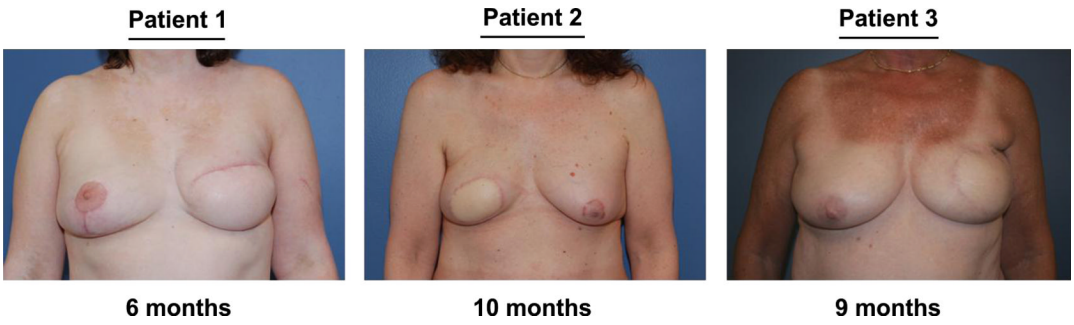

FIGURE 5.
Postoperative clinical images. All 3 women underwent unilateral delayed or immediate DIEP flap microsurgical reconstruction. Photographs shown were taken during postoperative follow-up at 6 months (patient 1), at 10 months (patient 2), and at 9 months (patient 3).

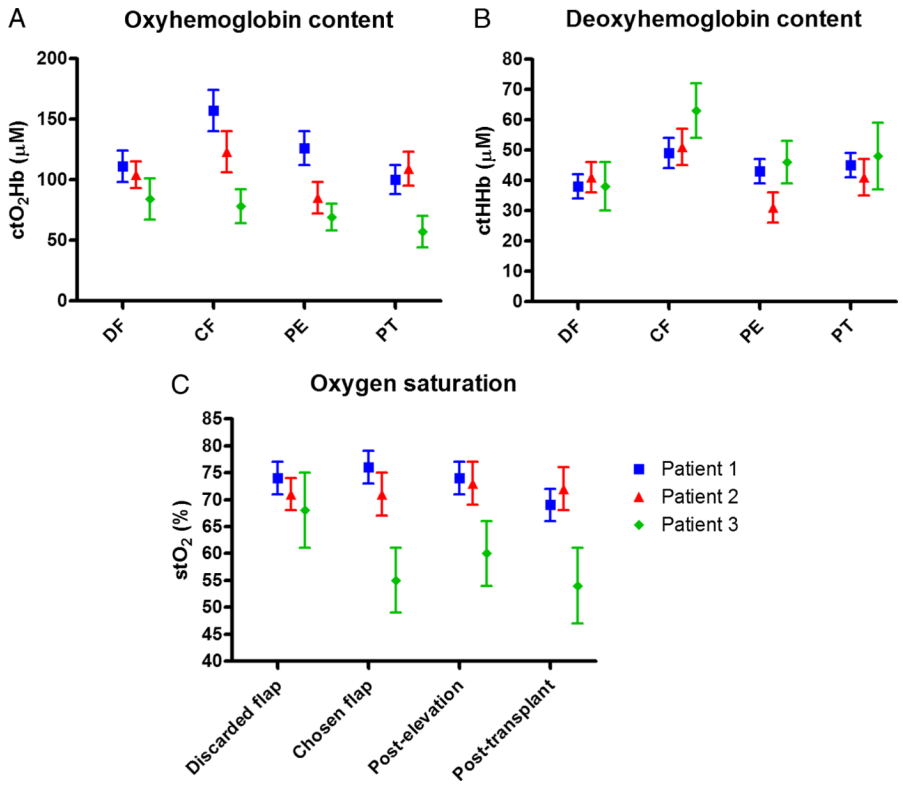

FIGURE 6.

Quantification of SFDI oxygenation imaging results. Localized measurements from similar regions of interest were quantified and their mean and standard deviation plotted. (A) Tissue oxyhemoglobin content, (B) tissue deoxyhemoglobin content, and (C) tissue oxygen saturation levels were evaluated for all 3 patients.

TABLE 1

Patient Demographics

Patient No.	Age, y	Reconstruction Timing	Location of the Perforator	Flap Weight, g
1	41	Delayed	2 lateral and 1 medial perforators	890
2	55	Immediate	1 lateral row perforator	326
3	65	Immediate	2 medial and 1 lateral perforators	524